Where were the Caribbean mangroves during the Last Glacial Maximum? A microtopographical approach

Valentí Rull

Spanish National Research Council (CSIC), Botanic Institute of Barcelona, Pg. del Migdia s/n, 08038 Barcelona, Spain. Email: vrull@csic.es

Institut Català de Paleontologia Miquel Crusafont (ICP-CERCA), Universitat Autònoma de Barcelona, c/Columnes s/n, 08193 Cerdanyola del Vallès, Barcelona, Spain. Email: valenti.rull@icp.cat

Abstract

During the Last Glacial Maximum (LGM), when global sea levels dropped by ~132 m, the Caribbean continental shelf was fully exposed, which drastically reduced the flat topographical habitat necessary for mangrove growth. It has been proposed that mangroves survived in flat microsites beyond the shelf break and later expanded from these microrefugia to their current distribution after the LGM. However, this hypothesis remains untested. This study aims to identify potential refugia by locating flat areas around the -132 m isobath using Global Multiresolution Topography (GMRT) images. A significant ~200-km-long potential refugium was identified on the northern Trinidad (NT) shelf, along with several scattered kilometer-scale microrefugia near the Cariaco Basin (CB) in northeastern Venezuela. Additionally, two isolated prospective microrefugia were detected in northern Colombia (NC) and western Hispaniola (WH). The remaining LGM Caribbean coasts were considered unsuitable for mangrove growth. The NT refugium, along with the CB microrefugia, may have served as the primary sources for subsequent mangrove expansion. This expansion was likely facilitated by postglacial sea-level rise and the SE-NE Caribbean Current (CC), which would have acted as a major agent for propagule dispersal. This microtopographical survey not only supports the microrefugial hypothesis but also narrows the focus to the most promising areas, significantly reducing the time, effort and resources required for future seismic and coring campaigns.

Keywords

Caribbean Sea, mangroves, Last Glacial Maximum, postglacial recolonization, (micro)refugia, sea-level rise

1. Introduction

Mangroves are tropical and subtropical intertidal forested ecosystems that are vital for maintaining coastal biodiversity, providing a range of ecological services, and serving as the most significant blue-carbon ecosystems, contributing to the mitigation of global warming. These ecosystems are among the most endangered on Earth (Worthington et al., 2020). Recent assessments indicate that global mangrove coverage has decreased by 3.4% in less than 25 years (1996–2020) due to both natural and human-induced deforestation (Bunting et al., 2022). If these depletion rates continue, mangroves face a significant risk of substantial decline during this century, posing a serious threat to their long-term survival (Duke et al., 2017).

Mangroves thrive around the average sea level, forming vegetation gradients that range from coastal marine habitats to the upper limits of normal tides in continental environments. They are especially well-developed in extensive, flat sedimentary areas, such as deltas or carbonate platforms, where wave action is weak or absent (Thom, 1984; Schaeffer-Novelli et al., 2002; Mazda et al., 2007). In contrast, mangroves do not develop in non-flooded or topographically complex environments, such as steep coastal slopes, rocky substrates, or littoral cliffs. A recent review by Ellison et al. (2024) reports that mangroves worldwide occupy elevation ranges between -0.90 and 3.60 m (-0.12 and 1.25 m on average) and extend inland from a few hundred meters to ~15 km (average 3.26 km). According to these data, the mean slope of flat areas (FAs) supporting mangroves ranges between 0.01% and 0.45% (average 0.12%), representing 35% to 267% (average 78%) of the total tidal range.

In the Caribbean region (Fig. 1), mangroves cover a total area of approximately 14,700 km², accounting for ~10% of the world's mangrove surface (Bunting et al., 2022). They are distributed along all Caribbean coasts, with the largest extents found in Cuba, Venezuela, Colombia, and Panama (1,500–3,600 km²). In contrast, all other countries have mangrove areas of 600 km² or less, with 15 countries having less than 100 km². The primary mangrove-forming trees in the region include the red mangrove (*Rhizophora*, Rhizophoraceae), black mangrove (*Avicennia*, Acanthaceae), and white mangrove (*Laguncularia*, Combretaceae). Additional components, such as the tea mangrove (*Pelliciera*, Tetrameristaceae) and the mangrove fern (*Acrostichum*, Pteridaceae), are also typical but occupy marginal environments.

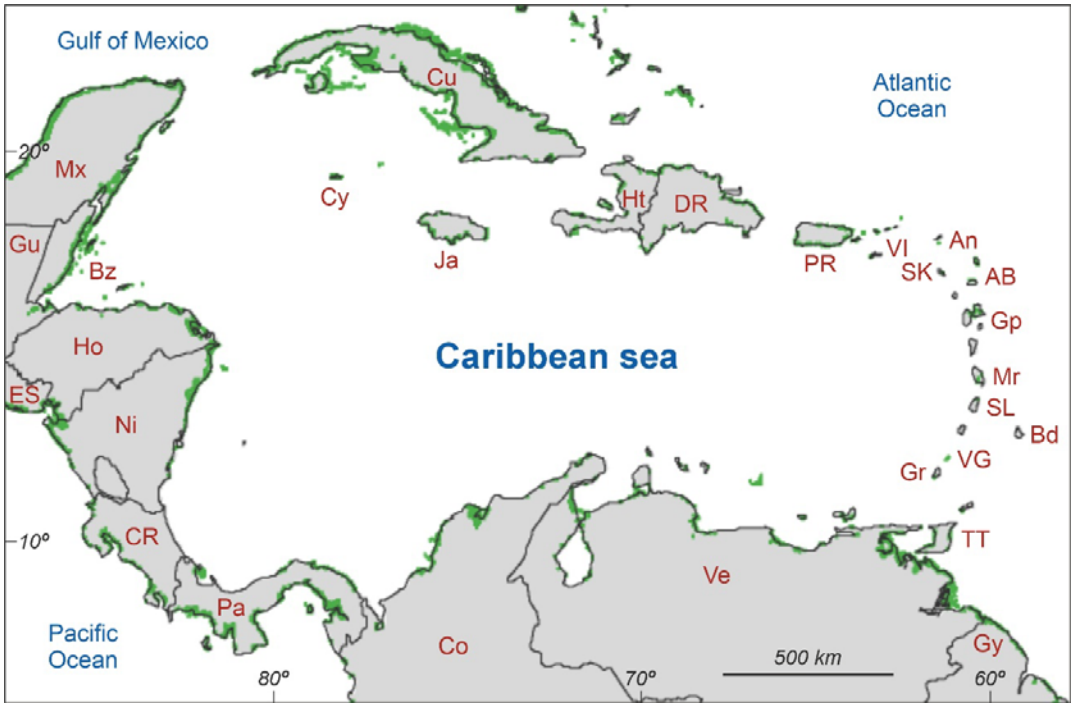

Figure 1. Map of the Caribbean mangroves (green patches), according to Bunting et al. (2022). Downloaded from NASA Landsat 5-TM (https://earthobservatory.nasa.gov/images/47427/mapping-mangroves-by-satellite). Countries/islands: AB, Antigua & Barbuda; An, Anguilla (UK); Bd, Barbados; Bz, Belize; Co, Colombia; CR, Costa Rica; Cu, Cuba; Cy, Cayman Islands (UK); DR, Dominican Republic; ES, El Salvador; Gp, Guadeloupe (France); Gu, Guatemala; Gy, Guyana; Ht, Haiti; Ja, Jamaica; Mr., Martinique (France); Mx, Mexico; Ni, Nicaragua; Pa, Panama; PR, Puerto Rico; SK, Saint Kitts & Nevis; SL, Saint Lucia; TT, Trinidad & Tobago; Ve, Venezuela; VG, Saint Vincent & The Grenadines; VI, Virgin Islands (USA/UK)

The Caribbean mangroves originated during the Middle Eocene (50–40 Ma) and were initially dominated by *Pelliciera* until the Eocene-Oligocene transition (EOT), when *Rhizophora* became the primary mangrove-forming tree. The Neogene marked a period of diversification, culminating in the current mangrove composition during the Pliocene. Throughout this time, mangrove evolution and biogeography were heavily influenced by regional tectonics, including the movement of the Caribbean plate, continental drift, and climatic/eustatic changes, such as the EOT cooling and associated sea-level fall. In the Quaternary, external drivers included the Pleistocene glacial/interglacial cycles and human activities, which began to have a regional impact around 6–5 ka. The detailed evolutionary history of mangroves can be found in Rull (2024a).

Pleistocene paleoecological records of in situ Caribbean mangroves are rare. The oldest such record, found on an exposed Jamaican terrace, consists of mangrove root scars dated to ~130 ka (MIS 5e highstand), a period when sea levels were several meters higher than today (Mitchell et al., 2001). Another record, from the Cariaco Basin (Fig. 2), dates to the Last Glaciation (approximately 68–28 ka), encompassing Heinrich Events H6 to H3 (González et al., 2008; González & Dupont, 2009). This record, obtained from a depth of 900 m, shows pollen of *Rhizophora* and *Acrostichum* consistently contributing less than 4% of the total pollen assemblage. Notably, there is a gap in the records that includes the Last Glacial Maximum (LGM; 27–19 ka; Clark et al., 2009). The next in situ record of mangroves, dominated by *Rhizophora* and *Avicennia*, corresponds to the earliest Holocene (12.4–11.8 ka) in the Orinoco Delta (Pocknall & Jarzen, 2024). As such, the LGM remains absent from Caribbean mangrove records.

During the LGM, global relative sea levels (RSL) were 130–134 m below present levels (Lambeck et al., 2014; Spratt & Liesecki, 2016). This substantial drop exposed large portions of continental shelves worldwide, which typically reach maximum depths of ~200 m (IHO, 2019). The exposure of these shelves likely had a significant impact on mangrove distribution, as most mangroves today grow on flat upper shelf environments, while LGM coastlines were located near or on steeper continental slopes, which are topographically unsuitable for mangroves. In the Caribbean, it has been hypothesized that LGM mangroves persisted in microrefugia beyond the shelf break in areas with favorable microenvironmental conditions. From these refugia, mangroves are thought to have expanded along Caribbean coasts during the postglacial sea-level rise, ultimately reaching their current distribution (Rull, 2024b). However, this hypothesis remains untested due to a lack of suitable paleoecological records.

To identify these potential LGM mangrove refugia, a high-resolution bathymetric survey is required to locate suitable FAs around the LGM-RSL. This study aims to identify these FAs around -132 m (the midpoint of the -130 to -134 m range) using a microtopographical bathymetric approach. This survey can help set the bases for understanding the biogeographical patterns of LGM mangroves and their subsequent range shifts during the Late Glacial and Holocene, leading to their present-day distribution. In addition, it is able to identify the best prospects for further coring campaigns aimed at locating the LGM mangrove communities using paleoecological methods, notably pollen analysis.

2. Study site and methods

2.1. Overview of the Caribbean seafloor

The Caribbean seafloor is a deep and complex surface shaped by the tectonic dynamics of the Caribbean microplate, located between the North and South American plates and the Pacific Cocos and Nazca plates (Mann, 2021). It is subdivided into four major basins, arranged from west to east: the Yucatan Basin (~4,350 m maximum depth), the Colombian Basin (~4,160 m), the Venezuelan Basin (~5,630 m), and the Grenada Basin (~3,000 m) (Fig. 2). These basins are separated by three significant submarine elevations: the Nicaraguan Rise, the Beata Ridge, and the Aves Ridge. The deepest point in the Caribbean is the Cayman Trench (~7,690 m), part of the Cayman Basin, which is separated from the Yucatan Basin by the Cayman Ridge.

The most extensive continental shelves are found along the western and southern coasts, particularly in the regions of Honduras/Nicaragua and the northwestern and northeastern coasts of Venezuela, including Trinidad and Tobago. The least extensive continental shelves are along the Mexican Caribbean coast, as well as the coasts of Costa Rica, Panama, northern Colombia, and north-central Venezuela. Among the islands, Cuba, Puerto Rico, and the northernmost and southernmost Lesser Antilles have notable continental shelf extents relative to their sizes. In contrast, for most other islands, the shelf break is located close to their coasts or just a few kilometers offshore. There is a strong correlation between the extent of continental shelves and the occurrence of mangroves, as evidenced by a comparison of Figures 1 and 2.

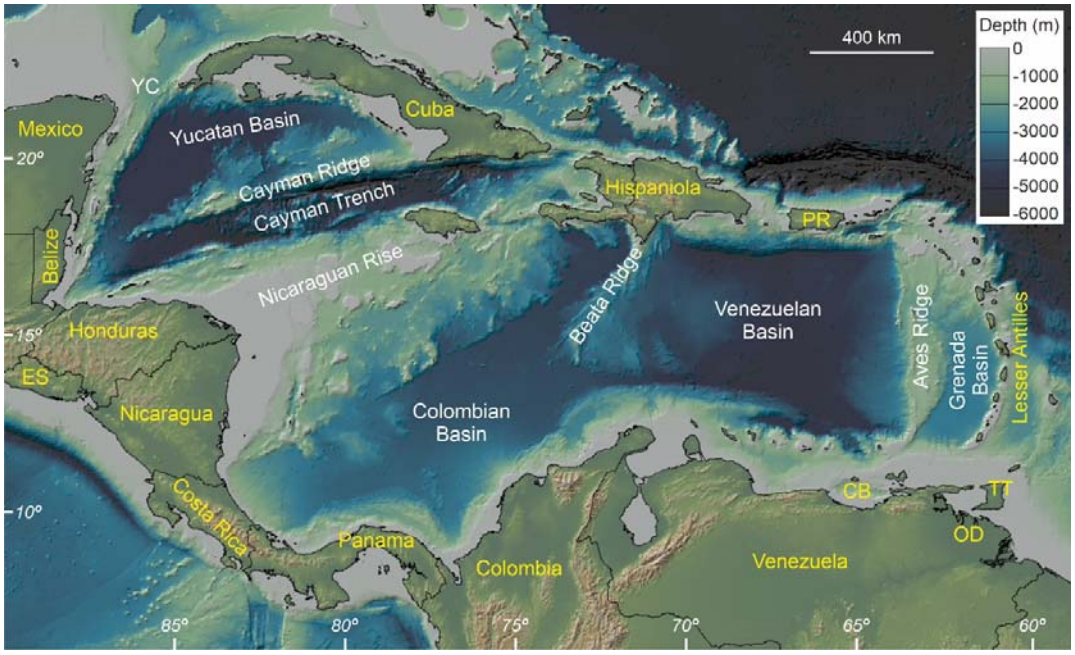

Figure 2. Reference map for this study. Overview of the Caribbean seafloor using Global Multi-Resolution Topography (GMRT) (see methods). Abbreviations: CB, Cariaco Basin; ES, El Salvador; Ja, Jamaica; OD, Orinoco Delta; PR, Puerto Rico; TT, Trinidad & Tobago; YC, Yucatan Channel.

2.2. Bathymetric image analysis

This survey focuses on identifying potential FAs for mangrove growth during the Last Glacial Maximum (LGM) lowstand using high-resolution bathymetric data. The primary tool for this analysis is the Global Multi-Resolution Topography (GMRT) dataset (Ryan et al., 2009), version 4.3.0, accessed through GeoMapApp 3.7.4 (www.geomapapp.org). This platform is hosted by the Lamont-Doherty Earth Observatory of Columbia University (USA) under a Creative Commons Attribution Noncommercial Share Alike 3.0 license. The analysis considers both horizontal (bathymetric contours) and vertical (land-sea elevation profiles) components and is conducted at three resolutions: macrotopographic, mesotopographic, and microtopographic.

The macrotopographic analysis utilizes the -132 m contour to delineate the portion of the continental shelf exposed during the LGM. Meso- and microtopographic analyses focus on a meter-scale depth range around this contour to identify FAs more suitable for mangrove growth. The depth range for meso- and microtopographic analyses was determined based on tidal amplitude.

The Caribbean is generally considered a microtidal region, with a tidal range below 20 cm (Kjerfve, 1981; Torres & Tsimplis, 2011). However, local variations exist, with maximum amplitudes of up to 2.6 m recorded along the Orinoco Delta coasts (Warne et al., 2002). During the Holocene, models suggest that Caribbean tidal ranges remained relatively stable, except around 9 ka, when tidal amplitudes reached 1–1.5 m along the western coasts near the Yucatan and Colombian basins (Hill et al., 2011; Khan et al., 2017). For the LGM, some modeling studies propose that tidal amplitudes in the Caribbean were similar to those of today (Thomas & Sündermann, 1999), while others estimate increases of 0.5–1 m along the Central American coasts (Egbert et al., 2004).

These dimensions align with the elevation ranges for mangrove gradients reported globally by Ellison et al. (2024), which extend up to 4.5 m, with average slopes of 0.12% (0.01–0.45%). Of this range, 20% or less lies below mean sea level. For an average LGM-RSL of -132 m, this corresponds to a gradient from approximately -128 m (upper mangrove limit; UML) to -133 m (lower mangrove limit; LML) over an average distance of 4.17 km (minimum 1.11 km). These conditions maximize the likelihood of identifying larger FAs suitable for mangrove growth while minimizing the chance of overlooking smaller but favorable FAs.

In the first step of this analysis, prospective FAs were identified as areas where the meter-scale isobaths from -128 to -133 m were more widely spaced. For this mesotopographic analysis, the Caribbean region between 8° and 23° N latitude and 60° to 90° W longitude was divided into 30 zones measuring 3° x 5° each (see Supplementary Material). Steep coasts and cliffs were identified as thin lines, reflecting tightly clustered isobaths along the same paths. In contrast, prospective FAs appeared as thick lines or dark spots, indicating wider isobath spacing over larger surfaces. In the second step, the microtopographic analysis, the identified prospective areas were magnified and examined in detail for the -128 to -133 m interval. This analysis used both isobaths and land-sea profiles and was compared against the elevation gradients reported by Ellison et al. (2024).

3. Results

3.1. Macrotopography

During the LGM, the shallow (<100 m) and discontinuous Caribbean continental shelf was mostly exposed (Fig. 3). The greatest exposure occurred in southern Cuba, the Nicaraguan Rise, and the northwestern and northeastern coasts of Venezuela, including Trinidad. In contrast, areas where the continental shelf is absent or where the shelf break lies close to the coast—such as Mexico/Belize, the Panama Isthmus, north-central Venezuela, and Hispaniola (Haiti and the Dominican Republic)—experienced minimal exposure. The Nicaraguan Rise is the only submarine elevation with exposed areas located far from present-day coasts.

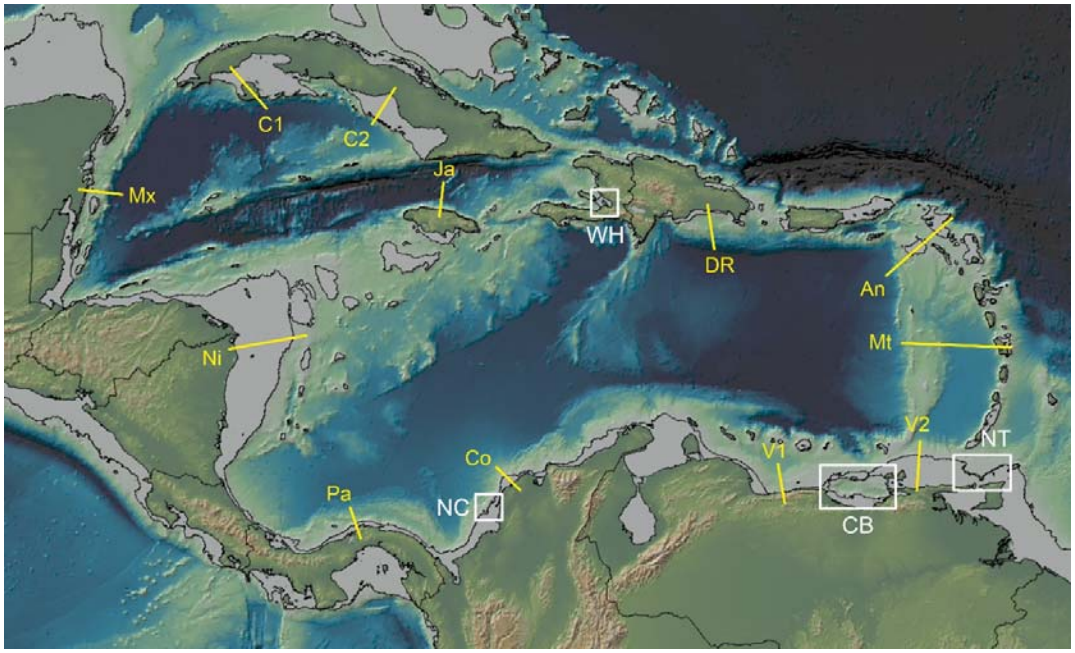

Figure 3. Map showing the -132 m contour (black line beyond the current coasts), the location of the land-sea elevation profiles displayed in Fig 4 (yellow lines) and the most prospective areas resulting from mesotorpographical analysis (white boxes), which are magnified in Figs. 5-7. Base map as in Fig. 2. Profiles: An, Anguilla; Co, Colombia; C1 and C2, Cuba; DR, Dominican Republic; Ja, Jamaica; Mt, Martinique; Mx, Mexico; Ni, Nigaragua; Pa, Panama; V1 to V3, Venezuela. Prospective areas: CB, Caariaco Basin; NC, northern Colombia; NT, northern Trinidad; WC, western Hispaniola.

A set of land-sea elevation profiles was selected around the Caribbean coasts to better visualize the submarine macrotopography of the continental shelf and slope (Fig. 4). The exposed shelf extends more than 100 km offshore in areas such as Cuba, northeastern Venezuela/Trinidad, and Nicaragua, where the shelf break is abrupt, the continental slope is steep, and the transition is continuous. In contrast, regions like Mexico and the Dominican Republic have a narrower exposed shelf, typically only a few tens of kilometers wide. The slope in these areas is composite, featuring two major steps separated by an intermediate plateau between approximately 1,200 and 1,800 m. In regions with high coastal ranges exceeding 2,000 m, such as north-central Venezuela, there is no significant shelf, and the continental slope directly continues from the mountain slope. The most complex profiles are found along the easternmost Caribbean coasts, where the shelf is fragmented in the Lesser Antilles, and the abyssal zone is interrupted by the Aves Ridge, as seen near Anguilla and Martinique.
In all cases, the LGM-RSL was located offshore, beyond the shelf break.

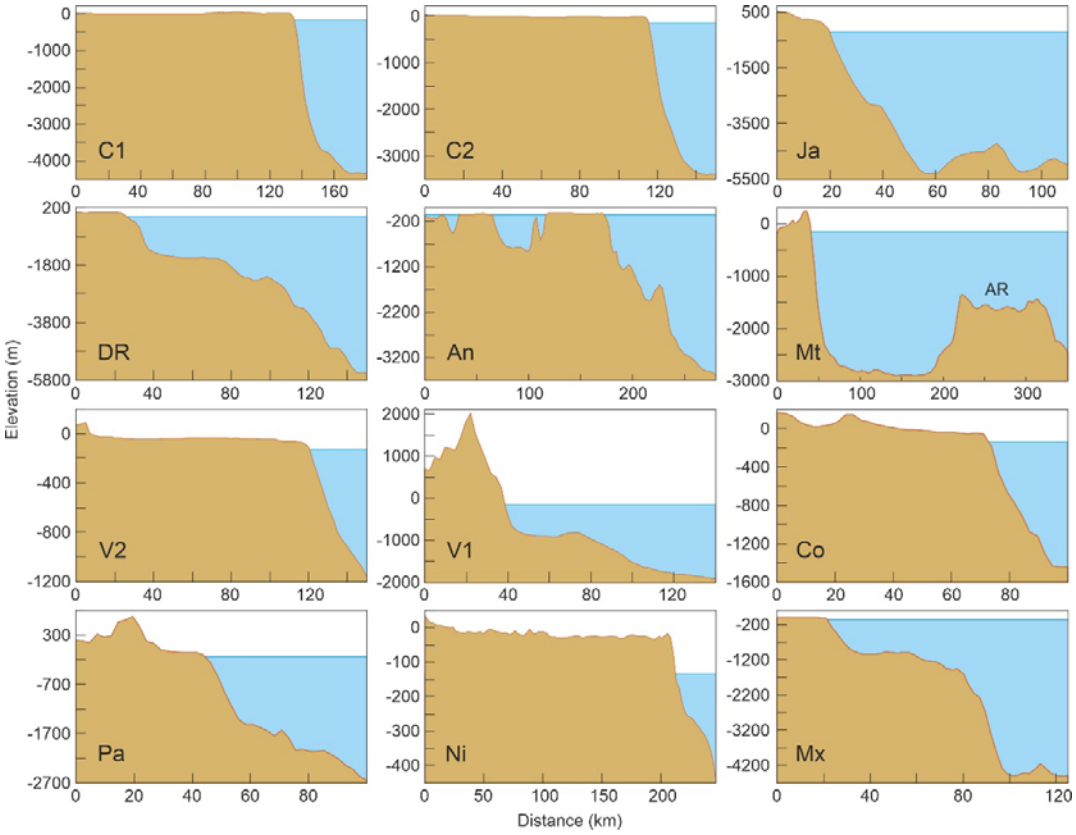

Figure 4. Distance-elevation profiles across the transects depicted in Fig. 3, showing the continental shelf/slope topography (brown areas) and the LGM sea level (blue) areas. Abbreviations: An, Anguilla; Co, Colombia; C1 and C2, Cuba; DR, Dominican Republic; Ja, Jamaica; Mt, Martinique (AR, Aves Ridge); Mx, Mexico; Ni, Nigaragua; Pa, Panama; V1 to V3, Venezuela.

3.2. Meso- and microtopography

The FA prospective sites identified in the mesotopographic analysis (Supplementary Material) were grouped into four main zones: the northern Trinidad shelf (NT), the Cariaco Basin (CB), the northern Colombian shelf (NC), and western Hispaniola (WH) (Fig. 3). The largest of these zones is NT, where the prospective FAs extend over approximately 200 km. The other zones consist of a few smaller spots, each less than 10 km wide. Along the remaining Caribbean coasts, the -128 to -133 m isobaths appear as thin lines, indicating steep coasts or coastal cliffs.

In the NT zone, FAs suitable for mangrove growth are more extensive in the central area, decreasing toward the east and west, where the coasts become steeper. This is illustrated by a central land-sea elevation profile (NTC), where the UML and LML span nearly 6 km inland with an average slope of 0.09% (Fig. 5). In contrast, an example of an unfavorable topographical gradient is found on the western side (NTW), where the UML and LML are less than 200 m apart, with an average slope of 3.05%. This slope is approximately 25 times the global average (0.12%) and seven times the maximum (0.45%) slope recorded worldwide for mangrove growth. A range of intermediate situations exists across the NT site, including slopes close to the maximum, as shown in an eastern profile (NTE) with an average slope of 0.41% between the UML and LML.

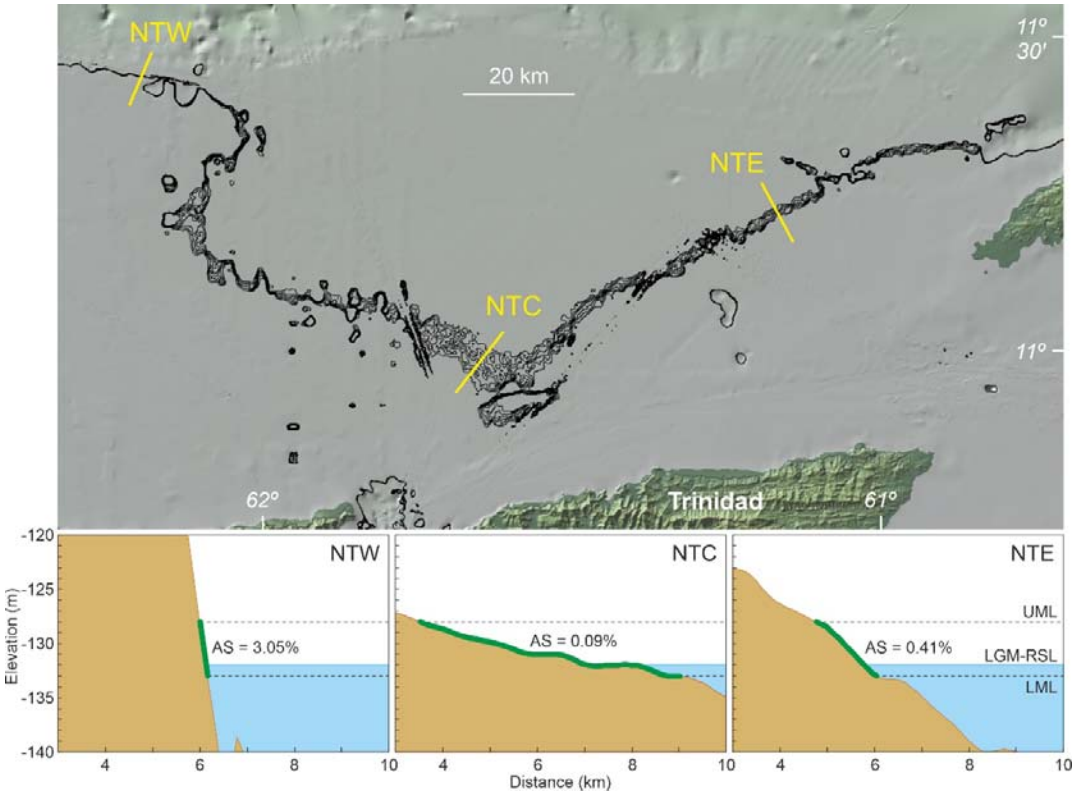

Figure 5. Close up of the NT site (Fig. 3) showing the isobaths between -128 and -133 m at meter resolution, and representative examples of LGM coastal profiles (yellow lines) from west to east. The space available for mangrove growth is highlighted by a thick green line in the below profiles. Abbreviations: AS, average slope; LGM-RSL, relative sea level during the Last Glacial Maximum; LML, lower mangrove limit (-133 m); UML, upper mangrove limit (-128 m).

In the CB zone, three small spots were identified, each within the slope range suitable for mangrove growth: 0.15% (CBN), 0.20% (CBS), and 0.24% (CBW) (Fig. 6). The remaining coasts in this zone appear as thin lines, resembling the steeper NTW profile in northern Trinidad. At the CBW site, the coastal profile is more complex than a single slope, and certain areas, particularly in the center of the profile, may be too steep for mangrove growth.

In the NC zone, two prospective sites were identified. The flatter site is located in the south (NCS; 0.17%), while the steeper site, though still within the mangrove range, is in the north (NCN; 0.28%) (Fig. 7). The WH zone presents a unique case. While the profile meets the conditions for mangrove growth, with slopes ranging from 0.23% in the northwest to 0.36% in the southeast, it is a closed basin—likely a coastal lagoon—of unknown water salinity.

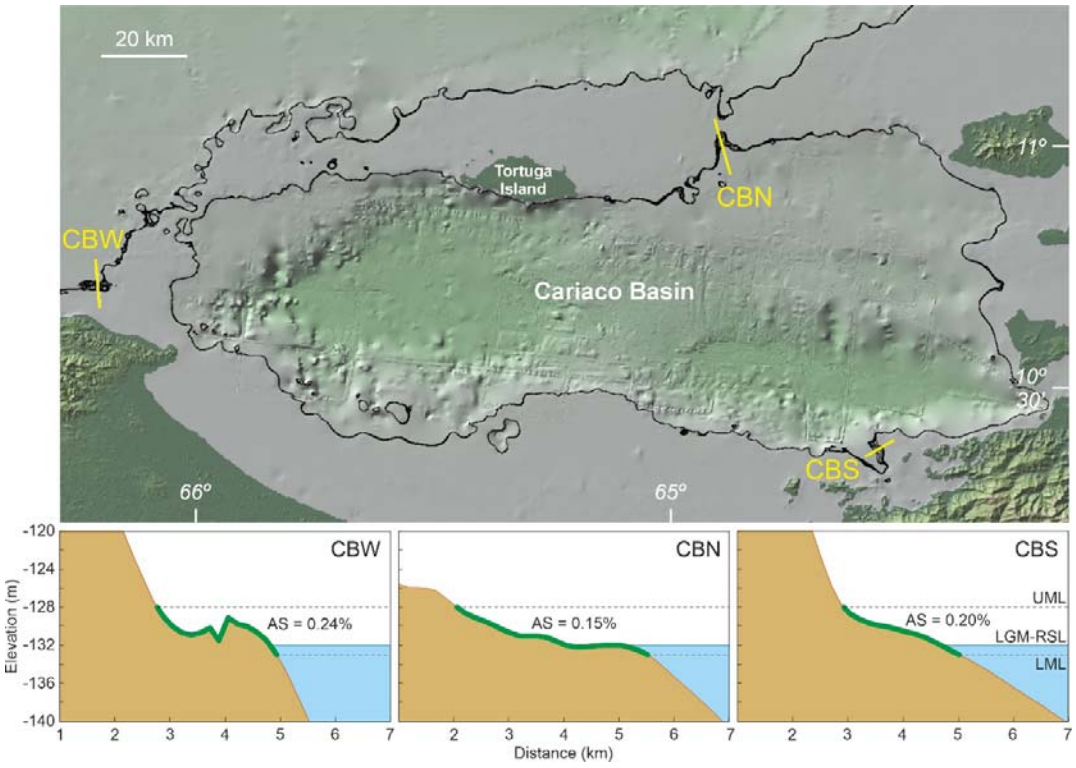

Figure 6. Close up of the CB site (Fig. 3) showing the isobaths between -128 and -133 m at meter resolution and the land-sea profiles cross the prospective sites identified (yellow lines). The space available for mangrove growth is highlighted by a thick green line in the below profiles. Abbreviations: AS, average slope; LGM-RSL, relative sea level during the Last Glacial Maximum; LML, lower mangrove limit (-133 m); UML, upper mangrove limit (-128 m).

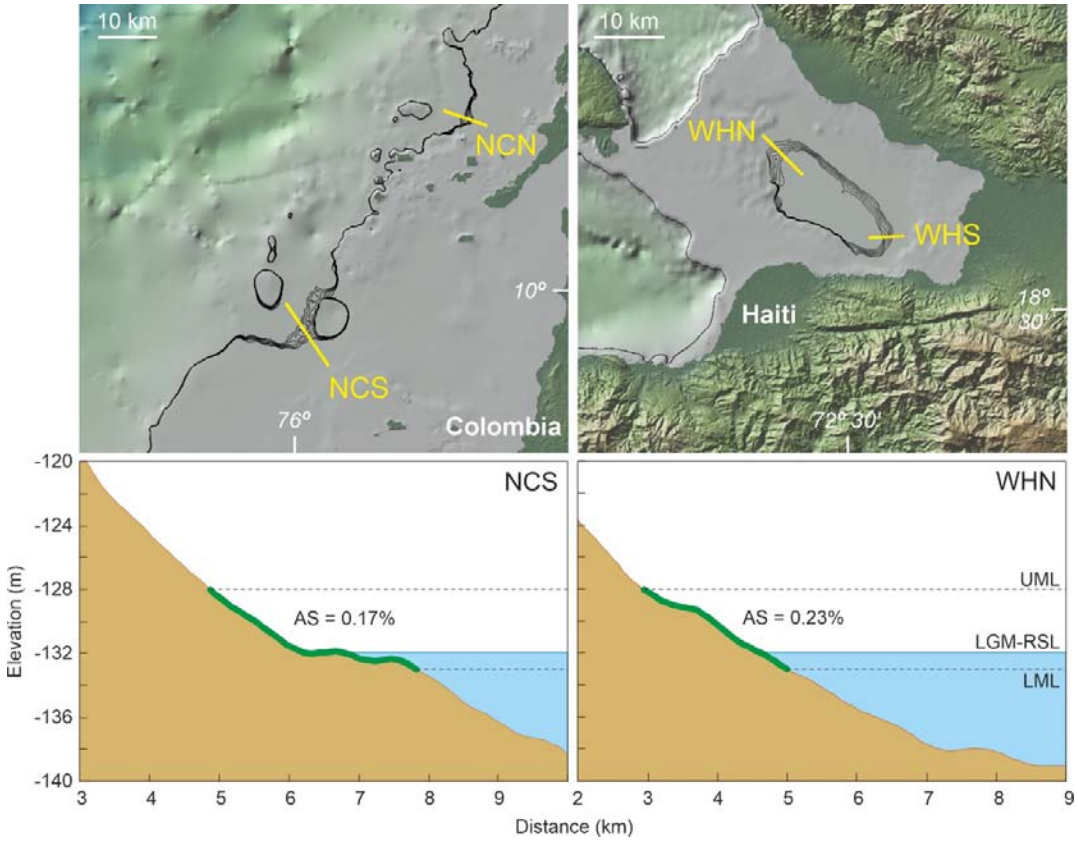

Figure 7. Close up of the NC and WH zones (Fig. 3) showing the isobaths between -128 and -133 m at meter resolution and the land-sea profiles across the prospective sites identified (yellow lines). The space available for mangrove growth is highlighted by a thick green line in the below profiles. Abbreviations: AS, average slope; LGM-RSL, relative sea level during the Last Glacial Maximum; LML, lower mangrove limit (-133 m); UML, upper mangrove limit (-128 m).

Conclusions and discussion

The results indicate that during the LGM, most Caribbean coasts were unsuitable for mangrove growth due to the aerial exposure of flat continental shelves and the steep land-sea elevation gradients typical of continental slopes. However, some zones remained where mangroves could have survived, considering the characteristic topography associated with these ecosystems. The largest accumulation of mangroves likely existed on the northern Trinidad shelf (NT), which may be considered the primary LGM mangrove refugium. Other topographically suitable areas consisted of small (km-scale) and scattered sites that fall under the category of microrefugia (sensu Rull, 2009).

Interestingly, the areas suitable for mangrove growth during the LGM were concentrated along the South American Caribbean coasts, particularly in the southeastern Caribbean region (northern Trinidad and northeastern Venezuela). No suitable FAs were identified along the remaining coasts, except for the western Hispaniola site, which was likely a coastal lagoon. This suggests that during the postglacial sea-level rise, mangroves may have colonized the entire Caribbean coastline primarily from refugia and microrefugia located in the southeastern region. Given that surface coastal currents are the main agents for dispersing mangrove propagules, especially in the Caribbean and other tropical regions worldwide (Van der Stocken et al., 2019), understanding the surface circulation patterns during the LGM is essential to evaluate the consistency this hypothesis, though not the hypothesis itself.

Currently, surface currents enter the Caribbean through the eastern coasts via the Northern Equatorial Current (NEC) and the Guyana Current (GC). The first flows through the Lesser Antilles, while the second enters through northern Trinidad and the Cariaco Basin (Fig. 8). Inside the Caribbean Sea, these currents form the Caribbean Current (CC), which flows in an ESE-NW direction before entering the Gulf of Mexico through the Yucatan Channel (Giry et al., 2013; Osborne et al., 2014; Felis et al., 2015). Isotopic evidence and modeling suggest that during the postglacial and Holocene sea-level rise, the general circulation patterns remained similar to those observed today, with minor variations in intensity and seasonality (Giry et al., 2013; Gu et al., 2017). Therefore, surface circulation would have been favorable for westward mangrove expansion from the primary LGM refugial areas in northern Trinidad and the Cariaco Basin across the Caribbean. Minor contributions from other microrefugia are also consistent with this circulation pattern.

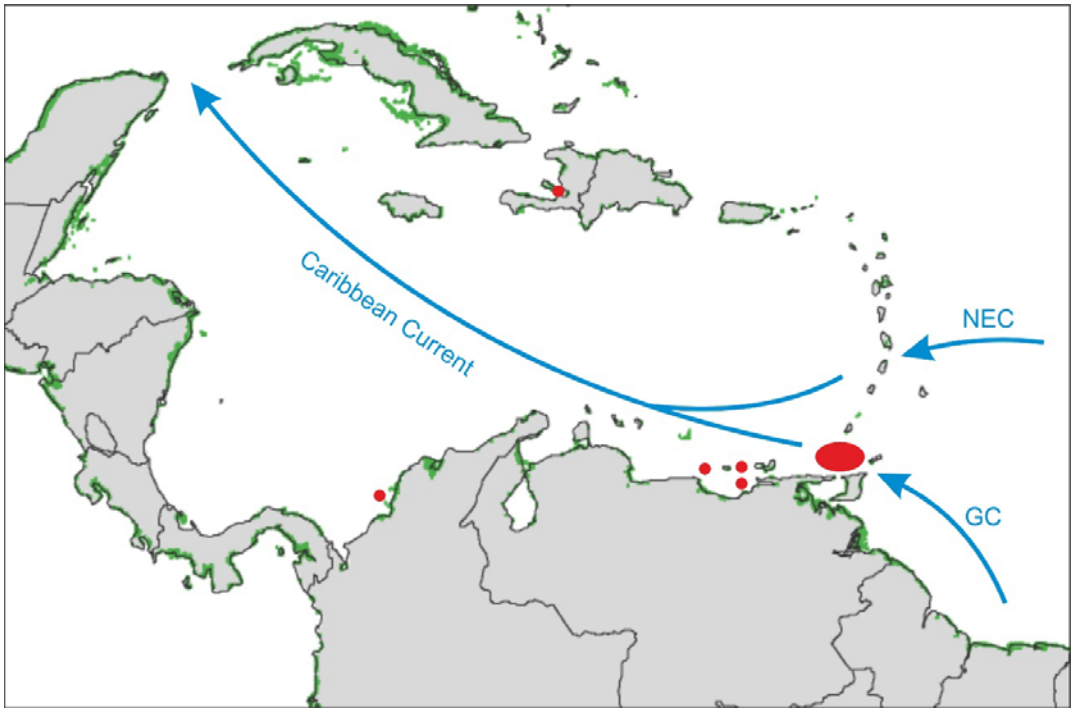

Figure 8. Map showing current mangrove areas as in Fig. 1 (green patches), the LGM refugial areas identified in this work (red dots) and the main superficial Caribbean currents (blue arrows). See text for more details. NEC, Northern Equatorial Current; GC, Guyana Current.

It should be emphasized that the occurrence of FAs around -132 m, as identified in this study, represents a minimum requirement for LGM mangrove persistence. Other critical environmental factors for mangrove growth, such as salinity, hydroclimate, river discharge, and sediment supply, can only be determined through paleoecological surveys involving marine coring. This study focuses on identifying the most promising paleoecological prospects, significantly reducing the area for potential LGM mangrove investigations and saving considerable time, effort, and resources.

According to the study results, the highest priority should be given to the northern Trinidad shelf, especially its central area (Fig. 5), which hosts the most extensive refugial site identified. This region could have been the primary inoculation zone for modern Caribbean mangroves following the LGM bottleneck that severely reduced mangrove extent. Coring in the NT

prospect and nearby offshore sediments is strongly recommended to elucidate mangrove dynamics during the LGM. The final selection of specific coring targets should be guided by seismic surveys of Pleistocene sediments. The proximity of gas fields and the associated facilities and infrastructures (NGC, 2023) could be of help in this sense.

The Cariaco Basin is a classical Neotropical site for Quaternary paleoclimate and paleoenvironmental reconstruction and has been intensively studied and cored. However, LGM sediments, if present, have not yet been analyzed—or results have not been published—for vegetation reconstruction and mangrove occurrence. The scarcity of mangrove pollen in slightly older sediments (68–28 ka; González et al., 2008; González & Dupont, 2009) may reflect the microrefugial nature of the surrounding sites (Fig. 6). Nonetheless, palynological analysis of potential LGM intervals in these sediments is recommended. Other potential microrefugial areas, such as NC and WH, also merit coring. In the NC zone, deeper offshore sediments should be targeted, while in WH, the best prospect appears to be the lagoonal depocenter. As with NT, seismic profiles would aid in identifying precise coring targets.

With the current information, alternative mangrove sources for colonization outside the Caribbean cannot be ruled out. For instance, the Guyana Current may have transported propagules from the Atlantic coasts; however, the existence of LGM mangrove refugia along these coasts remains unconfirmed. The Pacific coasts of Central America are separated from the Caribbean by a land barrier that would have been difficult for littoral ecosystems to cross, particularly under lowstand conditions. The Gulf of Mexico is also an unlikely source for Caribbean mangroves, as surface currents flow in the opposite direction. These hypotheses require further study to establish a consistent regional framework. In addition to paleoecological research, phylogenetic studies of extant mangroves could help inferring the geographical origin of current Caribbean mangroves.

Acknowledgments

No financial support was required specifically for the development of this work. The author is grateful to Andrew Goodwille for recommending the use of the GMRT tool for image analysis. The CERCA Programme, Generalitat de Catalunya, is also acknowledged.

References

Bunting,P., Rosenkvist, A., Hilarides, L., Lucas, R.M., Thomas, N. 2022. Global Mangrove Watch: updated 2010 mangrove forest extent (v2.5). Remote Sensing 14, 1034.

Clark, P.U., Dyke, A.S., Shakun, J.D., Carlson, A.E., Clark, J., Wohlfarth, B., et al. 2009. The Last Glacial Maximum. Science 325, 710-714.

Duke, N., Meynecke, J.-O., Dittmann, S., Ellison, A.M., Anger, K., Berger, U., et al. 2017. A world without mangroves? Science 317, 41-42.

Egbert, G.D., Ray, R.D., Bills, B.G. 2004. Numerical modeling of the global semidiurnal tide in the present day and in the last glacial maximum. Journal of Geophysical Research 109, C03003.

Ellison, J.C., Buffington, K.J., Thorne, K.M., Gesch, D., Irwin, J., Danielson, J. 2024. Elevations of mangrove forests of Pohnpei, Micronesia. Estuarine, Coastal and Shelf Science 268, 107780.

Felis, T., Giry, C., Scholz, D., Lohmann, G., Pfeiffer, M., Pätzold, J., et al. 2015. Tropical Atlantic temperature seasonality at the end of the last interglacial. Nature Communications 6, 6159.

Giry, C, Felis, T., Kölling, M., Wei, W., Lohmann, G., Scheffers, S. 2013. Controls of caribbean surface hydrology during the mid- to late Holocene: insights from monthly resolved coral records. Climate of the Past 9, 841-858.

González, C., Dupont, L.M. 2009. Tropical salt marsh succession as sea-level indicator during heinrich events. Quaternary Science Reviews 28, 939-946.

González. C., Dupont, L.M., Behling, H., Wefer, G. 2008. Neotropical vegetation response to rapid climate changes during the last glacial period: palynological evidence from the cariaco Basin. Quaternary Research 69, 217-230.

Gu, S., Liu, Z., Zhang, J., Rempfer, J., Joos, F., Oppo, D.W. 2017. Coherent response of Atlantic Intermediate Water and Atlantic Meridional Overturning Circulation during the last deglaciation: reconciling contrasting Neodynium isotope reconstructions from the tropical Atlantic. Paleoceanography 32, 1036-1053.

Hill, D.F., Griffiths, S.D., Peltier, W.R., Horton, B.P., Törnqvist, T.E. 2011. High-resolution numerical modeling of tides in the western Atlantic, Gulf of Mexico, and Caribbean Sea during the Holocene. Journal of geophysical Research 11, C10014.

IHO. 2019. Standardization of Undersea Feature Names. International Hydrographic Organization, Monaco.

Khan, N.S., Ashe, E., Horton, B.P., Dutton, A., Kopp, R.E., Brocard, G., et al. 2017. Drivers of Holocene sea-level change in the Caribbean. Quaternary Science Reviews 155, 13-36.

Kjerfve, B. 1981. Tides of the Caribbean Sea. Journal of Geophysical Research 86, 4243-4247.

Lambeck, K., Rouby, H., Purcell, A., Sun, Y., Sambridge, M. 2014. Sea level and global ice volumes from the Last Glacial Maximum to the Holocene. Proceedings of the national Academy of Sciences USA 111, 15296-15303.

Mann, P. 2021. Gulf of Mexico, Central America, and the Caribbean. In: Alderton, E., Elias, S.A. (eds.), Encyclopedia of Geology. Academic Press, London, pp. 47-67.

Mazda, Y., Wolanski, E., Ridd, P.V. 2007. The Role of Physical Processes in Mangrove Environments. TERRAPUB, Tokio.

Mitchell, S.F., Pickerill, R.K., Stemann, T.A. 2001. The Port Moran Formation (Upper Pleistocene, Jamaica): high-resolution sedimentology and paleoenvironmental analysis of a mixed carbonate clastic lagoonal succession. Sedimentary Gelogy 144, 291-306.

NGC. 2023. Energy Map of Trinidad and Tobago. The National Gas Company of Trinidad and Tobago Ltd., Port of Spain.

Osborne, A.H., Haley, B.A., Halthorne, E.C., Flögel, S., Frank, M. 2014. Neodynium isotopes and concentrations in Caribbean seawater: tracing water mass mixing and continental input in a semi-enclosed ocean basin. Earth and Planetary Science Letters 406, 174-186.

Pocknall, D.T. Jarzen, D.M. 2024. Biostratigraphic analysis of a Late Pleistocene to Holocene section from Punta Pescador, eastern Venezuela. Palynology 48, 2329582.

Rull, V. 2009. Microrefugia. Journal of Biogeography 36, 481-484.

Rull, V. 2024a. Origin and Evolution of Caribbean Mangroves. Springer Nature, Cham.

Rull, V. 2024b. The oldest Holocene caribbean mangroves and postglacial sea-level rise: biogeographical implications. Quaternary 7, 38.

Ryan, W.B.S., Carbotte, S.M., Coplan, J., O'Hara, S., Melkonian, A., Arko, R., et al. 2009. Global Multi-Resolution Topography synthesis dataset. Geochemsitry, Geophysics Geosystems 10, Q03014.

Schaeffer-Novelli, Y., Cintron-Molero, G., Soares, M.L.G. 2002. Mangroves as indicators of sea level change in the muddy coasts of the world. In: Healy, T., Wang, Y., Healy, J.-A. (eds.), Muddy Coasts f the World: Processes, Deposits and Function. Elsevier, Amsterdam, pp. 245-262.

Spratt, R.M., Liesecki, L.E. 2016. A Late Pleistocene sea level stack. Climate of the Past 12, 1079-1092.

Thom, B.G. 1964. Coastal landforms and geomorphic processes. In: Snedaker, S.C., Snedaker, J.G. (eds.), The Mangrove Ecosystem: Research Methods, UNESCO, Paris, pp. 3-17.

Thomas, M., Sündermann, J. 1999. Tides and tidal torques of the world ocean since the last glacial maximum. Journal of Geophysical Research 104, 3159-3183.

Torres, R.R., Tsimplis, M.N. 2011. Tides and long-term modulations in the Caribbean Sea. Journal of Geophysical Research 116, C10022.

Van der Stocken, T., Carroll, D., Menemenlis, D., Simard, M., Koedam, N. 2019. Global-scale dispersal and connectivity in mangroves. Proceedings of the National Academy of Sciences USA 116, 915-922.

Warne, A.G., Meade, R.H., White, W.A., Guevara, E.H., Gibeaut, J., Smyth, R.C., et al. 2002. Regional controls on geomrphology, hydrology, and ecosystem integrity in the orinoco Delta, Venezuela. Geomorphology 44, 273-307.

Worthington, T.A., zu Ermgassen, P.S.E., Friess, D., Krauss, K.W., Lovelock, C., Torley, J., et al. 2020. A global biophysical typology of mangroves and its relevance for ecosystem structure and deforestation. Scientific Reports 10, 14652.